

21世纪

学术研究文库

大连理工大学 生物医学工程 学术论文集

Proceedings on the Biomedical Engineering of
Dalian University of Technology

〔第2卷〕

邱天爽◎主编



大连理工大学出版社
Dalian University of Technology Press

大连理工大学生物医学工程学术论文集

(第 2 卷)

Proceedings on the Biomedical Engineering of Dalian
University of Technology
(Vol. 2)

主编 邱天爽

编辑委员会委员 雷明凯 唐一源
王 军 贺高红
娄 颖

大连理工大学出版社
2005 年 12 月

© 邱天爽 2005

图书在版编目(CIP)数据

大连理工大学生物医学工程学术论文集(第2卷) / 邱天爽主编. —大连:
大连理工大学出版社, 2005. 12

(21世纪学术研究文库)

ISBN 7-5611-2753-7

I. 大… II. 邱… III. 生物医学工程—文集 IV. R318-53

中国版本图书馆 CIP 数据核字(2005)第 150013 号

大连理工大学出版社出版

地址:大连市软件园路80号 邮政编码:116023

发行:0411-84708842 邮购:0411-84707961 传真:0411-84701466

E-mail: dutp@dutp.cn URL: http://www.dutp.cn

大连海事大学印刷厂印刷 大连理工大学出版社发行

幅面尺寸: 210mm×290mm 印张: 33.5 字数: 904千字

印数: 1~1000

2005年12月第1版

2005年12月第1次印刷

责任编辑: 吴孝东

责任校对: 于建辉

封面设计: 孙宝福

定 价: 130.00元(平装)

150.00元(精装)

序

在人类社会迈进 21 世纪之际,生命科学以前所未有的迅猛发展而受到人们的普遍关注和重视。特别是随着人类基因组研究、人类脑计划、生物芯片和克隆技术等新兴研究领域的发展和突破,生命科学越来越显示出其强大的生命力和不可比拟的重要性。可以这样说,21 世纪就是生物科学的世纪。

生物医学工程学科是综合生物技术、医学和工程学的理论和方法而发展起来的交叉性学科,是生命科学的重要支柱。生物医学工程的主要任务是运用工程技术手段,研究生物体特别是人体的结构、功能和其它生命现象,研究用于防病、治病、人体功能辅助及卫生保健的人工材料、制品、装置和系统,发展仿生工程科学的理论和技术。综观历史,生命科学的迅速发展,在很大程度上得益于生物医学工程各个技术领域的进步。17~19 世纪是生物医学工程的萌芽阶段,这个阶段的标志性成果是听诊器、体温计和血压计的问世,有力地促进了临床医学的发展;19 世纪末前后,伦琴发现了 X 射线,并且脑电图和心电图的研究也开始进行;20 世纪 60 年代以后,微电子和计算机技术的发展,有力地促进了生命科学和医学的进步,典型的标志性成果是 1971 年 CT 技术的诞生;近 20 年来,各种医疗仪器设备全面计算机化,伴随着产生了医疗技术的植入化、远程化和介入治疗技术,使现代医疗技术上上了一个台阶。

大连理工大学生物医学工程学科是近年来整合和发展起来的新学科,2003 年获得博士学位(一级学科)授予权和硕士学位授予权,2004 年建立了大连理工大学生物医学工程研究中心。大连理工大学生物医学工程学科覆盖了生物医学材料,生物医学信息检测与处理,生物医学成像与图像处理,生物医学系统建模与仿真和生物力学与康复工程等五个主要研究方向,有中国科学院院士 1 人,教授 24 人(含博士生导师 15 人),副教授 33 人,具有博士学位的教师 34 人。近年来,生物医学工程领域相关师生面向国际学术研究前沿和国民经济建设,承担和完成了包括国家 863、国家 973、国家自然科学基金在内的大量的科学研究和技术开发课题,以较快的速度发展,并在一些方向取得喜人的研究成果,有的达到国际先进水平。同时,生物医学工程学科还培养了一批博士和硕士研究生,并在教学和科研中锻炼了自己的队伍。

为了进一步推动大连理工大学生物医学工程领域的学科建设、科学研究和人才培养工作,进一步开展校内外和国内外相同及不同学科之间的交流与交叉,并展示大连理工大学生物医学工程学科的最新科研成果,在 2003 年编辑出版《大连理工大学生物医学工程学术论文集(第 1 卷)》的基础上,特组织编撰了这本《大连理工大学生物医学工程学术论文集(第 2 卷)》,相信它的问世,将促进我校生物医学工程学科的进一步发展。



2005 年 12 月

目 录

• 生物医学材料 •

- Biomedical properties of hydroxyapatite-based gradient coating on α - Al_2O_3 ceramic substrate
..... WANG Zhi-qiang, XUE Dong-feng, Lü Bing-ling, Henryk Ratajczak(3~12)
- Surface engineering of biomedical metallic materials by plasma-based low-energy ion implan-
tation ZHU Xue-mei, LEI Ming-kai(13~17)
- 相转化法制备聚氨酯多孔涂层 贵海芬,王昌明,赵红,齐民,杨大智(18~23)
- 羟基磷灰石涂层技术的研究进展 胡德平,姚再起,齐民(24~27)
- 冠脉支架表面 PLGA 涂层制备及其结合性能研究
..... 黄莹莹,张萌,刘洪泽,齐民,杨大智(28~31)
- 芫花二萜原酸酯类化合物对 DNA 拓扑异构酶 I 活性的抑制作用研究
..... 李晓娜,张凤鸿,宋其龄,张世轩(32~36)
- 区域选择性改性的纤维素衍生物作为生物材料表面的血液亲合性镀层材料 ... 刘春(37~43)
- γ -APS 改性不锈钢表面 PLGA 涂层在 hank's 模拟体液中的动态降解
..... 刘洪泽,赵红,齐民,杨大智(44~49)
- 口腔医用丙烯酸酯类粘接性单体的应用进展 刘慧,刘炼,张春庆(50~56)
- 医用高分子材料等离子体表面工程 刘洋,雷明凯(57~66)
- 近红外七甲川菁染料及其生物应用 舒凡,彭孝军,陈秀英(67~75)
- 血管支架非降解聚合物聚氨酯涂层制备与表征
..... 王昌明,黄莹莹,赵红,齐民,杨大智(76~79)
- 天然二萜原酸酯类抗癌活性物质芫花萜的波谱学研究
..... 张凤鸿,李晓娜,高秀娟,闻罗汉,张世轩(80~84)
- 不同材料花样冠状动脉支架抗压缩性能分析
..... 张庆宝,王伟强,梁栋科,齐民,杨大智(85~90)
- 医用不锈钢表面微孔丙交酯乙交酯共聚物薄膜的制备及其生物相容性研究
..... 赵红,邢滨,齐民,杨大智(91~95)

• 生物医学信息检测与处理 •

- 基于分数低阶矩的非高斯噪声中诱发电位提取新方法 查代奉,邱天爽(99~104)
- 基于稳定分布的超声图像散粒噪声抑制新方法 查代奉,邱天爽(105~111)
- 从生物医学文献中进行知识挖掘 林鸿飞,杨志豪,柴永春(112~118)
- 基于 LMSTDE 的胃电信号传播速率的估计
..... 刘文红,邱天爽,林志钺, Richard W. McCallum(119~124)
- 基于人工神经网络的癫痫棘波检测方法 邱天爽,初孟(125~132)
- 诱发电位中 α 稳定分布噪声参数的动态估计新方法 孙永梅,邱天爽(133~138)
- 一种基于分数傅立叶变换的棘波检测算法 田玉松,邱天爽(139~146)

- Liley 模型的模拟 EEG 信号的非线性预测和分析 王兴元, 谭贵霖(147~154)
- 医学超声图像分割的一种新方法 张启辉, 邱天爽, 刘颖(155~161)
- 人体脉搏波特征提取算法研究 周宽久, 陈雪峰(162~168)
- 新型脑电信号采集方法与应用研究 朱林剑, 包海涛, 孙守林, 梁丰(169~173)

• 生物医学成像与图像处理 •

- A coarse-to-refined approach of medical image registration based on combining mutual information and shape information
..... CHEN Wei-qing, OU Zong-ying, SONG Wei-wei(177~182)
- Automatic segmentation of virtual human organ based on improved color similarity coefficient LIU Bin, OU Zong-ying(183~190)
- A cone-beam algorithm based on nutating lines filtration for single circular trajectory
..... OU Zong-ying, WANG Yu, WANG Feng(191~197)
- 用脑功能成像的方法研究大脑的视觉成像机制 冯士刚, 唐一源(198~203)
- 指纹图像识别中的伪特征滤除算法研究 郭成安, 李建华, 王建永(204~213)
- 指纹图像细化处理的并行算法研究 郭成安, 王家隆(214~220)
- 放射治疗机最佳适形多叶组合光栅叶片形状设计 侯建华, 欧宗瑛, 宋卫卫(221~228)
- 基于亮度匹配的灰度医学成像着色算法 刘洪波, 王秀坤(229~232)
- 八叉树编码体数据的快速体绘制算法 宋涛, 欧宗瑛, 刘斌(233~239)
- 医学图像配准的某些进展 孙少燕, 唐焕文, 唐一源(240~245)
- 一种基于信息离散性度量的医学图像配准方法 孙少燕, 唐一源, 唐焕文(246~250)
- 事件相关功能磁共振成像实验设计的优化 王凯, 唐一源(251~256)

• 生物医学系统建模与仿真 •

- A prediction method with more precision on SARS epidemic transmission
..... JIANG Chong-li, CHE Yang-qiu, DONG Ming(259~262)
- Mathematical mechanism of quarantine measures for SARS epidemic
..... JIANG Chong-li, DONG Ming(263~269)
- Optimal control of SARS epidemics based on cybernetics
..... JIANG Chong-li, DONG Ming(270~279)
- A class of 2D graphical representation of DNA sequences
..... KANG Jin-hui, WANG Jun(280~285)
- Mathematic description of a simple penna model HE Ming-feng, YUE Hui(286~290)
- An evolutionary model based on bit-string with intelligence
..... HE Ming-feng, PAN Qiu-hui, YU Bing-lin(291~296)
- Modeling epidemic based on penna model
..... HE Ming-feng, PAN Qiu-hui, YU Bing-lin(297~303)
- Final state of a simple ecosystem HE Ming-feng, PAN Qiu-hui, WANG Shuang(304~317)
- A simple method for constructing phylogenetic tree
..... TANG Nan-nan, LI Chun(318~323)
- 基于元胞自动机的生物性病原物类疾病传播模型 贺明峰, 邓成瑞(324~329)
- 脑高级功能的量子信息模型的设想 靳静, 赵庆柏, 宋鹤山, 唐一源(330~333)
- 基于词典法和机器学习法相结合的蛋白质名识别
..... 李刚, 郭崇慧, 林鸿飞, 杨志豪, 唐焕文(334~339)

视觉信息等级处理的双脑协同性研究	李珊珊, 于庆宝, 冯士刚, 鹿麒麟, 唐一源	(340~343)
基于改进的神经网络方法预测 CTL 表位	刘涛, 宋哲, 刘伟	(344~351)
应用支持向量回归方法预测胎儿体重	刘子阳, 郭崇慧	(352~358)
PLS 方法应用于 T 细胞表位定量构效关系的研究	宋哲, 刘涛, 刘伟	(359~369)
SPM 的数学基础及其在脑功能成像研究中的应用	唐煊文, 潘丽丽, 唐一源	(370~377)
预言 fMRI 血氧水平依赖响应的信息处理模型	闫芬, 于庆宝, 冯士刚, 唐一源	(378~383)
想象能力研究概况	于庆宝, 隋丹妮, 李长军, 唐一源	(384~386)
蛋白质结构预测中的长程作用分析与研究	张红娟, 唐煊文	(387~392)
量子共振检测仪的应用	张雪, 侯耀芳, 唐一源	(393~397)

• 生物力学与康复工程 •

Applications of acoustic rhinometry in the modeling of living human nasal cavity based on CT scan		
LIU Ying-xi, ZHANG Jun, SUN Xiu-zhen, YU Shen, YU Chi, SU Ying-feng		(401~409)
富氧膜保健应用及其流道的研究	窦红, 贺高红, 王鹏宇	(410~417)
PLGA 微球注射剂的研究进展	高秀娟, 张世轩	(418~423)
河南蜂胶的化学成分研究	郭修晗, 赵伟杰, 王世盛	(424~426)
CA/PEI 螯合铜亲和膜吸附胆红素的初探	鞠佳, 贺高红, 陈兆安, 段志军	(427~432)
凝胶型 W/O/W 多重乳液担载胰岛素的前期研究		
	李丽娜, 贺高红, 丁路辉, 刘红晶	(433~439)
血管支架静力学模拟的建模简化方案	李宁, 顾元宪	(440~445)
HIV 逆转录酶非核苷抑制剂结合位点浅析	李悦青, 高志刚, 赵伟杰, 孟庆伟	(446~449)
参数识别在骨生长方程中的应用	刘迎曦, 张军, 赵文志, 孙秀珍	(450~455)
低应力环境对大鼠股骨的骨密度和几何形态学的影响		
	刘迎曦, 赵文志, 张军, 李守巨, 李靖年, 孙晓江	(456~459)
在不同应力环境下生长的大鼠股骨的生物力学试验研究		
	刘迎曦, 赵文志, 张军, 李守巨, 李靖年, 孙晓江	(460~464)
鼻腔结构形态对鼻腔气流的影响	刘迎曦, 于申, 孙秀珍, 苏英锋, 张军	(465~469)
非阿片类止痛药氟吡汀马来酸盐的制备及晶型调控和表征		
	孟庆伟, 周宇宇, 刘军, 赵伟杰	(470~474)
人体上呼吸道三维有限元重建与流场数值模拟	孙秀珍, 于驰, 刘迎曦	(475~480)
鼻腔结构的三维重建与气体流场数值模拟	孙秀珍, 于申, 刘迎曦, 郑朝攀, 张军	(481~485)
紫外辐射接枝法制备双重敏感性渗透分离膜	唐亮, 贺高红, 李印华, 林畅	(486~493)
平板膜分离器富氧过程的数学模拟	王鹏宇, 贺高红, 窦红, 李祥村	(494~497)
渗透压下 W/O/W 多重乳液的聚并研究	肖公奎, 刘红晶, 贺高红, 丁路辉	(498~503)
温莪术化学成分的研究	张金梅, 赵伟杰, 王世盛	(504~506)
膜分离技术及其在生物医药领域中的应用	张玲玲, 贺高红, 李祥村, 胡亮平	(507~512)
去除尿毒症患者体内尿素的乳化液膜稳定性的研究		
	赵国强, 贺高红, 刘红晶, 李丽娜, 丁路辉	(513~518)
海洋生物碱类药物研究进展(II)	赵伟杰, 王世盛, 孟庆伟, 李悦青	(519~525)

生物医学材料

Biomedical Materials

Biomedical properties of hydroxyapatite-based gradient coating on α - Al_2O_3 ceramic substrate

WANG Zhi-qiang^{1,2}, XUE Dong-feng¹, LV Bing-ling¹, Henryk Ratajczak³

- (1. State Key Laboratory of Fine Chemicals, Department of Materials Science and Chemical Engineering, School of Chemical Engineering, Dalian University of Technology, Dalian 116012, China;
2. Department of Material Science and Engineering, Dalian Institute of Light Industry, Dalian 116034, China;
3. Faculty of Chemistry, University of Wrocław, ul. F. Joliot-Curie 14, 50-383 Wrocław, Poland.)

Abstract: A hydroxyapatite-based gradient coating on α - Al_2O_3 ceramic substrate is prepared by a multi-layer slurry-dipping and sintering process, on the basis of the glass binder with the chemical composition Na_2O 8.0, K_2O 7.0, Al_2O_3 3.0, ZnO 1.5, B_2O_3 15.0, SiO_2 65.5 (wt%). The coating component varies gradually, in which hydroxyapatite increases and glass decreases gradually from the interface (between the coating and alumina substrate) to surface layer. The microstructure and mechanical properties of the coating layer can be effectively improved by the present design. The obtained gradient composite possesses a high hydroxyapatite concentration and porous surface, which thus leads to a good biocompatibility and bioactivity (e.g., the good biodegradation).

Key words: hydroxyapatite, coating, biomaterials, α - Al_2O_3 ceramic substrate

α - Al_2O_3 陶瓷衬底上羟基磷灰石基涂层材料的生物医学性能

王志强^{1,2}, 薛冬峰¹, 吕秉玲¹, Henryk Ratajczak³

- (1.大连理工大学 精细化工国家重点实验室, 化工学院, 辽宁 大连 116012;
2.大连轻工学院 材料化工系, 辽宁 大连 116034;
3. Faculty of Chemistry, University of Wrocław, ul. F. Joliot-Curie 14, 50-383 Wrocław, Poland.)

摘 要: 本文采用多层淤浆浸渍和烧结工艺, 在 α - Al_2O_3 陶瓷衬底上制备了羟基磷灰石基涂层, 其中, 涂层材料是以玻璃片为基底的, 基片的化学成分是 Na_2O 8.0, K_2O 7.0, Al_2O_3 3.0, ZnO 1.5, B_2O_3 15.0, SiO_2 65.5 (质量百分比)。最后制备的涂层材料的组分是均匀变化的, 从界面(涂层和衬底之间)到表面, 羟基磷灰石含量逐渐增加而玻璃基片逐渐减少。采用本文设计的工艺流程, 可以有效地改善涂层材料的微观结构和机械性能, 同时, 所获得的涂层组分拥有较高的羟基磷灰石梯度浓度和较大的比表面积, 从而使涂层材料有良好的生物适应性和生物活性(即良好的生物降解性能)。

关键词: 羟基磷灰石; 涂层; 生物材料; α - Al_2O_3 衬底

中图分类号: Q811.7

发表于: Journal of Non-Crystalline Solids 351, 1675-1681 (2005)。

基金项目: 高等学校全国优秀博士学位论文作者专项资金(编号 200322)。

作者简介: 薛冬峰(1968-), 男, 河南南阳人, 博士, 大连理工大学化工学院教授, 博士生导师, 主要研究方向为功能材料化学与化工等。 E-mail: dfxue@chem.dlut.edu.cn

1 Introduction

Hydroxyapatite ($\text{Ca}_{10}(\text{PO}_4)_6(\text{OH})_2$, abbreviated as HAP) is a kind of bioactive materials that attracts wide interests, which has a typical composition close to the nature bone, and thus possesses the excellent biocompatibility and bioactivity. It has been well studied that porous HAP has a function to induce the growth of bone, when it is implanted into the human body as the artificial bone. However, HAP ceramics have some weaknesses such as the poor toughness (1.0~1.2MPa) and low bending strength (50~150MPa). However, if the relative density of HAP ceramics is increased, their mechanical properties can be effectively increased, but the corresponding bioactivity will thus be decreased.

To prepare HAP coating on some substrates with the high toughness and strength (such as Ti, Ti-6Al-4V alloy and zirconia or alumina ceramics), is an efficient way to get superior biomaterials possessing both advantages of HAP and corresponding substrate (i.e., combining the good biocompatibility and bioactivity into the high toughness and strength^[1]). In practice, such a combination (of HAP with its substrates) is not so tight and durable when they are implanted into the organism, due to the thermal stress caused by the difference of thermal expansions between HAP and its substrate. Therefore, the idea of using gradient function materials is introduced into the biomaterials field, several kinds of gradient bioactive composites have been studied^[2-7]. Maruno et al.^[2-5] studied HAP-Glass-Ti gradient composite by the sintering process, however, the glass composition in HAP-Glass-Ti composite should be strictly controlled, since it has a relatively low softening point. Therefore, HAP-Glass gradient coating can only be sintered below 1000°C to effectively protect the oxidization of Ti (or Ti-6Al-4V alloy). On the other hand, the glass should not react with HAP during the sintering process, which limits the combination strength and other related properties of the composite. Other kinds of gradient coatings on Ti-6Al-4V substrate, such as those prepared by the plasma spray process have been reported^[8]. HAP decomposes into β -TCP [β -tricalcium phosphate, β - $\text{Ca}_3(\text{PO}_4)_2$] during the plasma spray process at high temperature, which thus accelerates the degradation of the coating when the composite is implanted into organizations. Ceramics such as zirconia or alumina can combine well with the glass flux, and allow the coating to be sintered at high temperature. Alumina ceramics possess excellent properties such as the high strength, good chemical durability and biocompatibility, which thus become a kind of excellent functional ceramic materials. The preparation and characterization of alumina-based HAP-Glass gradient coating are studied in the present work, with the aim to effectively modulate the microstructure and quality of gradient composites.

2 Experimental details

Alumina ceramics contain 5% (wt) CaO-MgO- Al_2O_3 - SiO_2 glass flux, the raw material is α - Al_2O_3 with the average particle size 0.3 μm . The size of glass flux powders is 200 mesh. The batch powder is obtained by a semi-dry pressing process at 200 MPa, and is then sintered at 1450°C for 2 hours. The ceramics are worked into a $\phi 20 \times 4\text{mm}$ disc.

HAP powders are synthesized by a wet route, using $(\text{NH}_4)_2\text{HPO}_4$ and $\text{Ca}(\text{NO}_3)_2 \cdot 4\text{H}_2\text{O}$ in the alcohol aqueous solution. HAP powders are fired at 1000°C and grinded to be 200 mesh (after cooling). The glass composition in the coating is Na_2O 8.0, K_2O 7.0, Al_2O_3 3.0, ZnO 1.5, B_2O_3 15.0, SiO_2 65.5 (wt%), the raw materials are soda, K_2CO_3 , lime, ZnO , H_3BO_3 , SiO_2 (AR). The glass is melted at 1450°C for 2 hours and then poured into water. The glass is grinded in an alcohol media and passes a 200 mesh screen after the filtration and drying.

HAP-Glass gradient coating is prepared on α -Al₂O₃ ceramic substrate by a multi-layer slurry-dipping and sintering process. Three kinds of gradient coatings are prepared in this work, their corresponding structures and components are collected in Table 1.

Table 1 Structures and components of three kinds of gradient coatings (wt%)

Sample Nos. & components	No. 1		No. 2			No. 3		
	HAP	Glass	HAP	α -Al ₂ O ₃	Glass	HAP	α -Al ₂ O ₃	Glass
Under layer	0	100	0	0	100	0	20	80
Second layer	30	70	20	20	60	30	10	60
Third layer	50	50	50	10	40	50	5	45
Surface layer	70	30	70	0	30	70	0	30

The gradient coating is prepared according to the following procedures. (1) to etch the surface of alumina ceramics by the mixture of HF 5% and HNO₃ 3%; (2) to apply the first layer, and the whole sample is fired at 1100°C for half an hour (after drying); (3) to etch the first layer surface by the mixture of HF 5% and HNO₃ 3% again, then the second layer is applied to the etched (first) layer, the whole sample is again fired at 1100°C for half an hour (after drying). The latter layers are obtained in the same way.

X-ray diffraction (XRD) patterns of the surface layer are measured using Cu K α by a diffractometer (Regagu Dmax-III). FTIR spectrophotometer (Nicolet 20DXB) is used to measure the IR absorption spectra of the powder to confirm whether HAP reacts with the glass or not during the firing process. The mixture of HAP (70 wt%) and glass (30 wt%) is sintered at 1100°C for half an hour, and is grinded into fine powders that are used for XRD and IR analyses. The morphology (i.e., the cross-section and surface analyses) of the coating is observed by a scanning electron microscope (SEM, KYKY-1000B).

The tensile strength (to characterize the bonding strength of the coating) is tested according to the method ASTM-C633. The alumina ceramic disc with HAP-Glass gradient coating is bonded to two metal stripes by the high strength adhesive, as shown in Fig. 1. A critical load F is measured when the coating is peeled off. The tensile strength σ_f is calculated by the equation $\sigma_f = F/S = 4F/\pi d^2$, where d is a diameter of the ceramic disc.

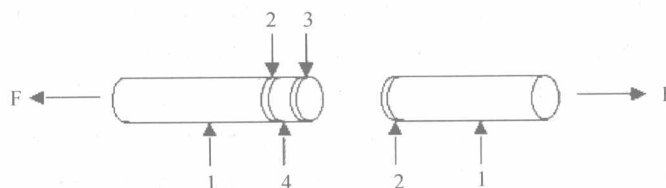


Fig. 1 Schematic drawing of the bonding strength test.

(1) metal stripe, (2) high strength adhesive, (3) gradient coating, (4) alumina ceramics.

Auto X-ray diffractometer with a rotation target (D/MAX-RC) is used to test the residual thermal stress in the coating by $\sin^2\psi$ method. The crystal plane (526) of HAP is selected as a characteristic plane, the diffraction angle is $2\theta = 141.352^\circ$, the angle ψ is fixed as 0° , 5° , 30° , and 45° , respectively. The residual thermal stress can be calculated by the formula,

$$\sigma_{\varphi} = \left[-\frac{E}{2(1+\nu)} (\operatorname{ctg} \theta_o) \frac{\pi}{180} \right] \frac{\partial 2\theta_{\varphi\psi}}{\partial \sin^2 \psi} = KM \quad (1)$$

In Eq. (1) M can be calculated when different $2\theta_{\varphi\psi}$ data are detected at different ψ values,

where K is a constant, and $K = -\frac{E}{2(1+\nu)} (\operatorname{ctg} \theta_o) \frac{\pi}{180}$.

σ_{φ} : the residual thermal stress;

φ : the angle between both directions of the residual thermal stress and axis X ;

E : the elastic modulus;

ν : Poisson's ratio;

$2\theta_o$: the diffraction angle of a certain crystal plane when no thermal stress is existed, in this

experiment $2\theta_o = 141.352^\circ$;

$2\theta_{\varphi\psi}$: the diffraction angle of a certain crystal plane when the thermal stress is existed;

ψ : the angle between the normal direction of a certain crystal plane and axis Z .

Intramuscular implantation experiments are carried out to study the biomedical properties of the current coating. Two kinds of cubic blocks with the compositions that are same as those of the surface and third layers of the gradient coating (where the surface layer consists of 70% HAP and 30% glass, the third layer consists of 50% HAP, 5% α - Al_2O_3 and 45% glass), are sintered in the same way as the preparation of the gradient coating. Two kinds of samples are labeled S (the surface layer) and T (the third layer), respectively. These blocks are worked into small samples with the size of about $2 \times 2 \times 2$ mm, 15 pieces of each kind of samples are selected to implant into 30 healthy white adult rats with the weight of about 25 g, which are offered by the animal center of the municipal central hospital of Dalian. These white rats are equally divided into two groups, one group is used to implant S samples, another group is used to implant T samples. Two side-legs of these rats are selected to give a local anesthesia, hairs are scraped off, two incisions at the outer side of two legs are made, the muscle is obtusely unripped and one piece sample is implanted into each side of legs. The rats are fed in a normal way after this operation, the general conditions of these rats such as normal activities, foods taking and wounds recovering are carefully observed. 3 rats from each group after this operation are killed after 24 h, 72 h, 2 weeks, 4 weeks, 8 weeks, respectively. The involved muscle of the implanted part is taken from the leg and treated with 4% polyformaldehyde (POM). After the de-calcium procedure, the muscle samples are embedded with paraffin, sliced up and colorized by the ordinary rule. The muscle specimens are observed by an optic microscope. The implanted samples are separated, immersed in deionized water for 24 h, washed 3 times with alcohol, dewater with acetone and dried at 110°C . The surface of these samples (after the implantation) is observed by the optic microscope and SEM, with the aim to find

their changes during the implantation.

3 Results

In our experiments, HAP-Glass gradient coating can be bonded to the substrate very well, no any breaking off or remarkable cracks appear when the coating is fired. The average bonding strengths (tested by a tensile tester as shown in Fig. 1) of the measured samples (labeled as Nos. 1, 2 and 3) are 32.9 MPa (standard error ~ 1.1 MPa), 46.4 MPa (standard error is ~ 1.4 MPa) and 48.2 MPa (standard error is ~ 1.2 MPa), respectively. The residual thermal stress in the coating is tested by $\sin^2\psi$ method, according to XRD results. The residual thermal stresses of different coatings (Nos. 1, 2 and 3) are calculated by the Eq. (1), their values are 43.7 MPa, 34.2 MPa, and 30.4 MPa (with the standard errors ~ 1.4 MPa, ~ 1.9 MPa, and ~ 1.2 MPa), respectively. These results agree well with the bonding strengths of these samples, where the high thermal stress corresponds to the low bonding strength. SEM image of the glass coating on alumina substrate is shown in Fig. 2, in which it can be found that the glass is well combined into the substrate.

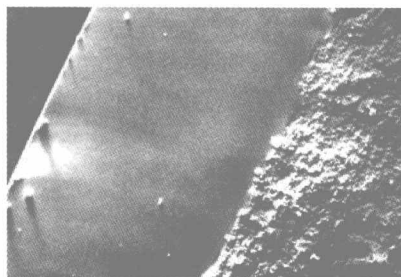
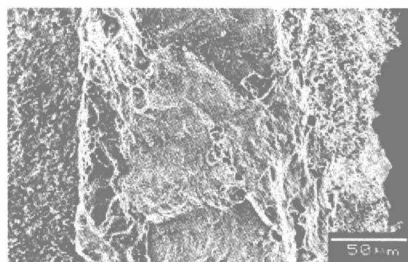
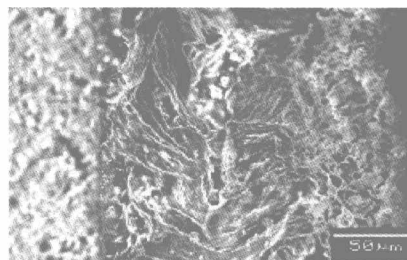


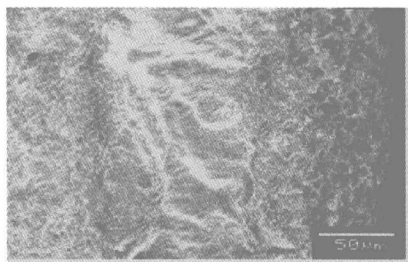
Fig. 2 SEM image of the first layer (the glass) adhered on alumina substrate ($\times 1000$).



(a) sample No. 1



(b) sample No. 2



(c) sample No. 3



(d) surface

Fig. 3 Cross section and surface microstructures of the as-prepared coatings with different compositions.

The cross section and surface microstructures of the obtained coatings are observed by SEM, as shown in Fig. 3. It can be found that these coatings possess an obvious gradient structure, i.e., the inner structure of the coating is dense, which become loose and porous from the interface (between the coating and substrate) to surface gradually. At the same time, EDS analysis also indicates that the composition of these coatings varies gradually from the interface to surface.

XRD patterns of the surface and second layers of the sample No. 3 are shown in Fig. 4, which show that the crystalline phase in the surface layer is HAP, and in the second layer is HAP and α - Al_2O_3 . FTIR spectra of the surface layer are shown in Fig. 5, in which it can be found that before sintering there are some absorption bands in the range of 3571.95cm^{-1} , 1090.07cm^{-1} , 1043.87cm^{-1} , 972.14cm^{-1} , 631.86cm^{-1} , 602.50cm^{-1} and 571.95cm^{-1} corresponding to the characteristic wave numbers of HAP, Si-O bands in the glass have the absorption bands at the wave numbers 945.48cm^{-1} and near $1060\sim 1070\text{cm}^{-1}$. -OH bands at 3571.95cm^{-1} and 631.86cm^{-1} are the characteristic wave numbers of HAP.

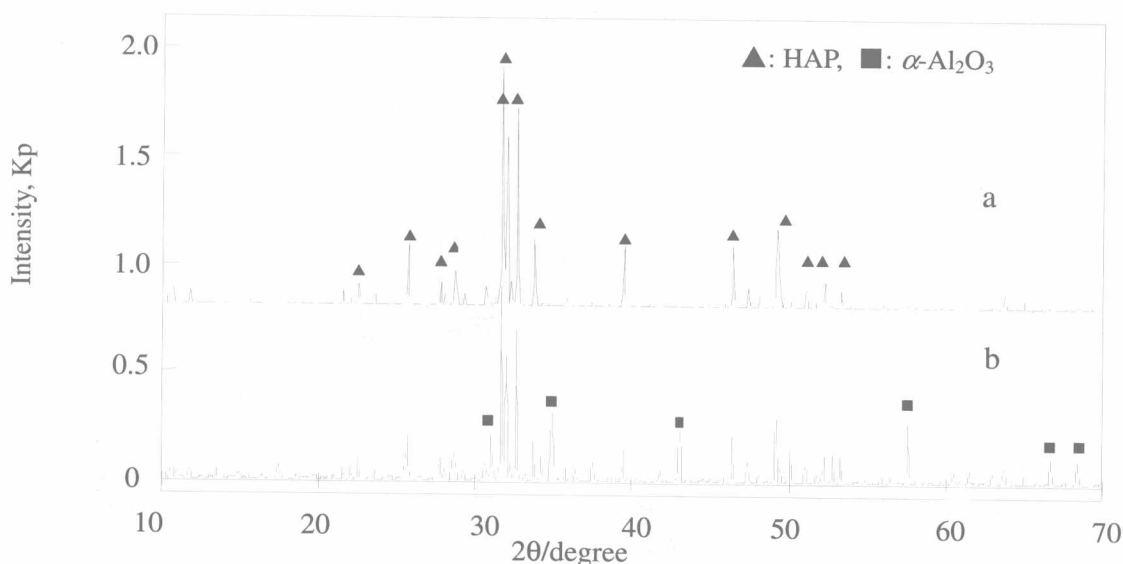


Fig. 4 XRD patterns of the surface and second layers.

(a) surface layer, 70 HAP and 30 glass (wt%); (b) second layer, 30 HAP, 10 α - Al_2O_3 , and 60 glass (wt%).

The linear scanning chemical analysis of Si and Ca elements in the No.3 coating is shown in Fig. 6, where the scanning range is marked in Fig. 3(c), which shows that the content of Si decreases gradually from the interface to surface, while the content of P increases gradually.

In the intramuscular implantation experiment, a small amount of macrophages can be found around the tissues near the implanted materials, which indicates that the implanted materials have the biodegradation (in a certain degree), SEM images also confirm this conclusion. SEM images show us clear changes of the surface structure of sample S in Fig. 7, in which it can be found that the surface becomes more porous and the pore size becomes larger with increasing the implantation time. SEM images of the sample T are shown in Fig. 8. It can be found that the surface structure of the samples with the composition of the third layer is more different from that of the surface layer, even it shows a certain change caused by the degradation, which is much less than that of the surface layer. Our present results indicate that the third layer is more stable than the surface layer, that is, the third layer has a better durability than the surface layer. This is due to the addition of α - Al_2O_3 in the composition.

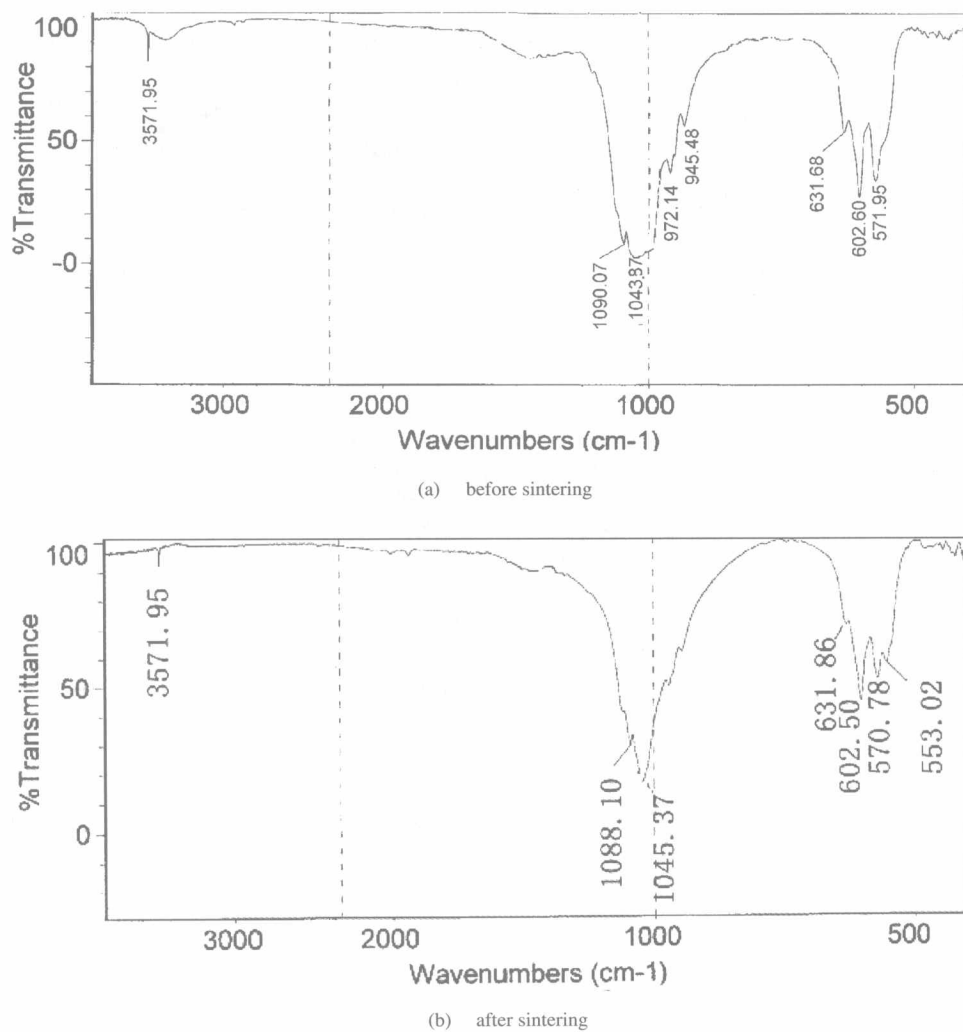


Fig. 5 FTIR spectra of the surface layer.

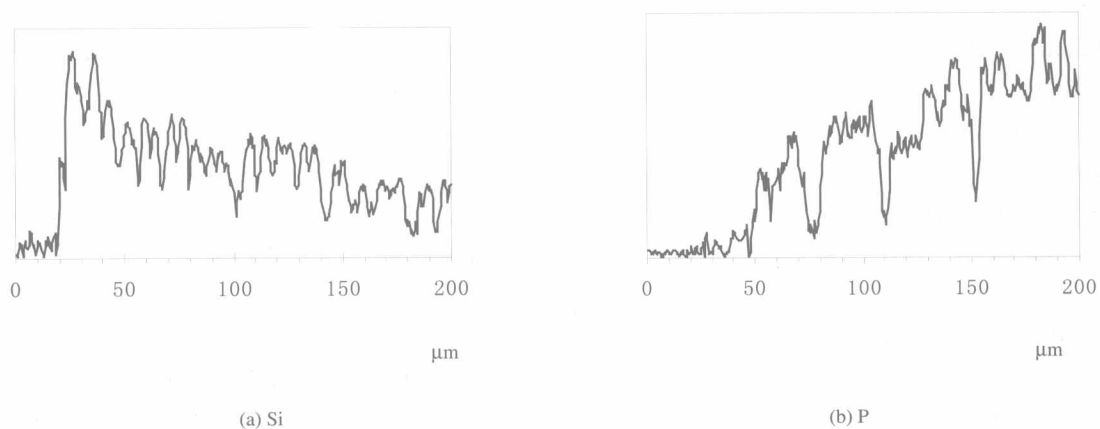


Fig. 6 Linear scanning chemical analysis of Si and P elements in the gradient coating

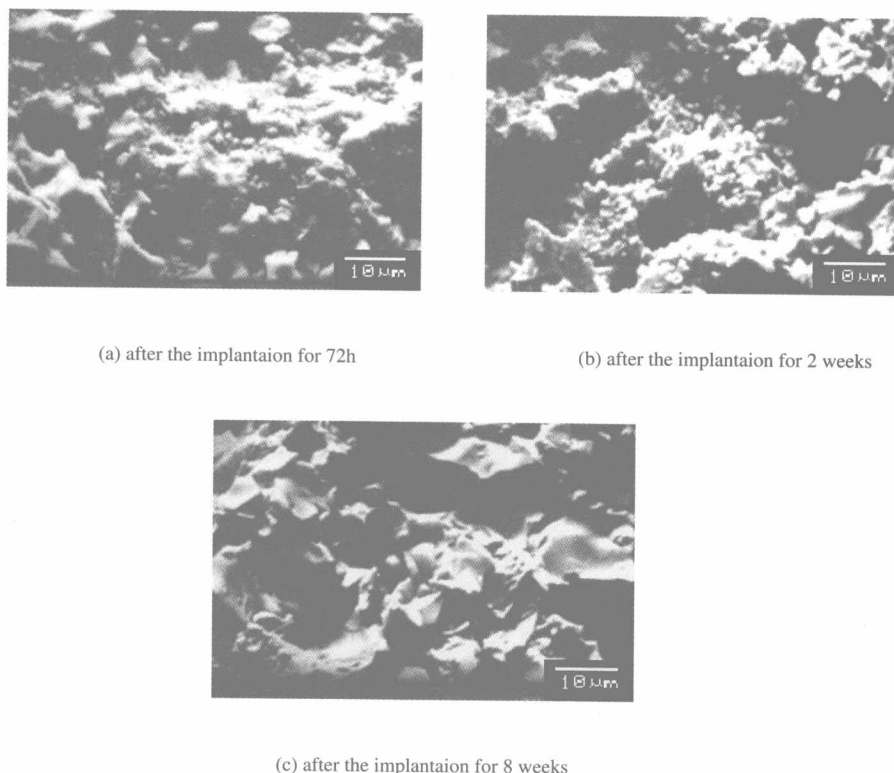


Fig.7 SEM images of the surface microstructures of sample S, which are implanted into the leg of white rats for different periods.

4 Discussion

The present strength is much higher than those when HAP bioactive film is coated on metal, alloy or ceramics. The difference between both thermal expansion coefficients of HAP ($\sim 14.0 \times 10^{-6}/^{\circ}\text{C}$) and substrate ($8.4 \times 10^{-6}/^{\circ}\text{C}$ for alumina ceramics, $8.71 \times 10^{-6}/^{\circ}\text{C}$ for Ti and $9.4 \times 10^{-6}/^{\circ}\text{C}$ for Ti-6Al-4V, respectively) may cause a big thermal stress when HAP coating is prepared on the substrate, which can lead to HAP film breaking off or cracking. In this work, the glass with a lower thermal expansion coefficient ($8.86 \times 10^{-6}/^{\circ}\text{C}$) is used in HAP-Glass gradient coating, which induces thermal expansion coefficients of the coating layer to vary gradually (increasing gradually from the interface between the coating and substrate to the surface), therefore, the thermal stress in such a gradient coating is lower than that in single HAP coating on metals or ceramics.

In these samples, No. 3 sample has the highest bonding strength and lowest thermal stress among our prepared coatings. Moreover, when the first layer (glass is dominant) is fired on alumina ceramics, alumina can effectively react with the glass, in other word, alumina and the liquid state glass can well diffuse each other. Such reasons may result in the current coating bonded to the substrate tightly.

As shown in Fig. 4, our results indicate that HAP is stable and just reacts with the glass slightly, HAP does not decompose during the sintering process. FTIR spectra in Fig. 5 also confirm our present conclusion. In Fig. 5(b) for the sample after sintering at 1100°C , we can find that $-\text{OH}$ bands at 3571.95cm^{-1} and 631.86cm^{-1} are very clear, which verify that the component of the surface layer contains HAP. On the other hand, it can be found that the band shift is caused by the glass composition.